than in the non-ARS group (91.6% vs. 58.7%, $P = 0.02$). Univariate Cox hazards analysis revealed that the presence of anti-ARS antibodies was associated with better prognosis (HR = 0.34, 95% CI 0.08–0.80; $P = 0.01$).

Conclusions

The presence of anti-ARS antibodies is a possible prognostic marker in patients with PM/DM-ILD.

Introduction

Idiopathic inflammatory myopathy (IIM) comprises a group of systemic autoimmune disorders, including polymyositis (PM) and dermatomyositis (DM), affecting skeletal muscles and other organs [1–3]. In patients with PM/DM, interstitial lung disease (ILD) is a common extramuscular involvement associated with poor prognosis [4–6]. We previously described the clinical features of ILD-associated PM/DM (PM/DM-ILD) [7, 8] and identified the prognostic factors based on the clinical characteristics of a large series of PM/DM-ILD patients [9].

Accumulating evidence supports an association between ILD and the presence of certain myositis-specific autoantibodies (MSAs); in particular, anti-aminoacyl tRNA-synthetase enzyme (ARS) antibodies and anti-melanoma differentiation-associated gene 5 (MDA-5) antibody (also termed anti-CADM-140 antibody) are more closely associated with ILD than other MSAs [10–15]. Anti-ARS antibodies were detected in approximately 50% of PM/DM-ILD patients [11]. To date, eight types of anti-ARS antibodies (Jo-1, PL-7, PL-12, EJ, OJ, KS, Zo, and Ha) have been identified [10, 16]. Although patients with different types of anti-ARS antibodies show some unique clinical features and prognosis [17–21], these patient subgroups can also present with similar clinical manifestations, such as ILD, myositis, arthritis, Raynaud's phenomenon, and "mechanic's hands" [also known as anti-synthetase syndrome (ASS)] [16, 17].

Yoshifuji *et al.* reported that the response to initial therapy is better in anti-ARS-positive PM/DM-ILD than in anti-ARS-negative PM/DM-ILD [11]. However, there have been no studies comparing the radiological and pathological features between anti-ARS-negative and anti-ARS-positive PM/DM-ILD patients or assessing the long-term prognostic significance of anti-ARS antibodies.

In contrast, several studies have demonstrated the clinical significance of anti-MDA-5 antibody, which is exclusively detected in DM or clinically amyopathic DM (CADM) [13–15, 17]. Patients positive for anti-MDA-5 antibody more often developed rapidly progressive and fatal ILD [13–15] compared with those positive for anti-ARS antibodies [15]. Anti-MDA-5 and anti-ARS antibodies are mutually exclusive [17]. Therefore, the early discrimination between patients positive for anti-ARS antibodies and anti-MDA-5 antibody is crucial for determining the appropriate treatment strategy for PM/DM-ILD.

At present, anti-MDA-5 antibody can be measured only in specialized facilities by protein immunoprecipitation tests or enzyme-linked immunosorbent assay (ELISA) [14, 17, 22]. Conversely, anti-ARS antibodies are measurable using a commercially available ELISA kit (MESACUP anti-ARS test, MBL, Nagoya, Japan) or a line blot assay kit (EUROLINE Myositis Profile 3, EUROIMMUN AG, Luebeck, Germany) [23]. We previously demonstrated that this ELISA kit can detect anti-ARS antibodies with sensitivity and specificity comparable to the RNA immunoprecipitation (RNA-IP) test [23]. Here using this ELISA kit, we aimed to describe the

clinical, radiological, and pathological features of PM/DM-ILD and compare the prognosis of anti-ARS-positive to anti-ARS-negative PM/DM-ILD patients.

Materials and Methods

Subjects

The institutional review board of Hamamatsu University School of Medicine approved this study (approval number 25–225) and waived patient approval or informed consent because the study involved a retrospective review of patient records, images, and pathological specimens. This information was notified on the website (http://hamamatsu-lung.com/study.html).

We retrospectively reviewed consecutive patients diagnosed with PM/DM-ILD between 1995 and 2013 at Hamamatsu University Hospital (Hamamatsu, Japan). Of the 56 patients identified, 8 were excluded because of overlapping connective tissue diseases (CTDs) (5 patients with Sjögren's syndrome, 1 with systemic sclerosis, 1 with rheumatoid arthritis, and 1 with systemic lupus erythematosus). There were no patients who had active malignancies at initial diagnosis. Finally, 48 PM/DM-ILD patients were included in this study.

The diagnosis of PM/DM was confirmed on the basis of Bohan and Peter's criteria [1, 2]. In this study, patients with definite or probable PM/DM were included. CADM was diagnosed as a distinct subgroup of DM when the patient had a skin rash characteristic of DM without the clinical evidence of muscle disease and with little or no increase in serum creatine kinase (CK) during the study period [3, 7, 9, 14, 15, 24].

ILD was diagnosed based on clinical presentation, pulmonary function tests, high-resolution computed tomography (HRCT) images, and lung biopsy findings [25–28]. All patients underwent transbronchial lung biopsy and/or bronchoalveolar lavage (BAL), and 27 patients (56%) also underwent surgical lung biopsy (SLB). Patients with other known causes of ILD were excluded [25–28].

Disease onset type was classified as ILD-preceding type if ILD diagnosis preceded PM/DM diagnosis by three months or longer, concomitant onset type if ILD and PM/DM were diagnosed within 3 months, or myositis-preceding type if PM/DM diagnosis preceded ILD diagnosis by 3 months or longer [4, 7]. ILD form was classified as acute/subacute (lasting less than 3 months from the onset) or chronic (lasting 3 months or longer) according to the clinical presentation [7, 9]. For the assessment of clinical course, improvement and deterioration of ILD were defined based on the International Consensus Statement of idiopathic pulmonary fibrosis (IPF) [28] with slight modification by the consensus of 2 lung physicians specializing in ILD. Briefly, improvement or deterioration were defined by two or more of the following: (1) a decrease or increase in respiratory symptom severity, (2) a decrease or increase in parenchymal abnormality on chest HRCT scan, and/or (3) a $\geq$10% increase or decrease in percent predicted forced vital capacity (%FVC) or a $\geq$10 Torr increase or decrease in arterial oxygen pressure (PaO_2).

Detection of anti-ARS antibodies

For all 48 PM/DM-ILD patients diagnosed at Hamamatsu University Hospital, the serum samples stored since the initial ILD diagnosis were available. The samples were screened using a recently developed ELISA kit (MESACUP anti-ARS test, MBL, Nagoya, Japan) that can detect five anti-ARS antibodies (Jo-1, PL-7, PL-12, EJ, and KS) [23]. If positive, the presence of anti-ARS antibodies was confirmed by RNA-IP [23].

Of the 48 PM/DM-ILD patients meeting the inclusion criteria, anti-ARS antibodies were detected in 24 using the ELISA kit, of which 23 were also anti-ARS-positive by RNA-IP (termed ARS group). The one patient positive for anti-ARS antibody by ELISA but negative by RNA-

IP, and the 24 patients negative for anti-ARS antibodies by ELISA were classified as negative; thus, 25 patients were classified as negative for anti-ARS antibodies (non-ARS group) (Fig. 1). Anti-ARS antibodies detected in this study included PL-7 in 8 patients, Jo-1 in 6, PL-12 in 4, KS in 2, EJ in 2, and KS + EJ in 1.

Review of radiographical findings

HRCT images acquired at initial ILD diagnosis were reviewed. These images comprised 1–2.5-mm collimation sections at 10-mm intervals. They were reconstructed by a high spatial frequency algorithm and displayed at window settings appropriate for viewing the lung parenchyma (window level, -600 to -800 Hounsfield units; window width, 1200 to 2000 Hounsfield units). Images were randomized and reviewed independently by two expert chest radiologists unaware of the related clinical information. The images were assessed for the presence and distribution of lung parenchymal abnormalities on HRCT findings.

The predominant distribution of abnormalities on HRCT findings was evaluated according to the following criteria. Cranio-caudal predominance was assessed as "upper" when most of the abnormal HRCT findings were above the level of the tracheal carina, as "lower" when most of the abnormalities were below the level of the tracheal carina, and as "random/diffuse" when most of the abnormalities were distributed randomly or diffusely. The axial distribution was classified as "peripheral" if the abnormalities were present primarily in the outer third of the lung, "peribronchovascular" if abnormalities were primarily around the bronchus and artery, and "diffuse" if abnormalities were distributed diffusely.

HRCT findings, including ground-glass opacity (GGO), consolidation, reticular opacity, honeycombing, traction bronchiectasis, non-septal linear opacity/subpleural curvilinear line (SCLL), emphysema, and lower lobe volume loss were interpreted according to Fleischner's criteria with slight modification [29] (S1 Protocol). Each CT finding was recorded as present or absent.

HRCT pattern was classified as usual interstitial pneumonia (UIP) pattern, possible UIP pattern, or inconsistent with UIP pattern according to the guidelines for IPF with slight modification [26]. The cases interpreted as inconsistent with UIP pattern were further classified as nonspecific interstitial pneumonia (NSIP) pattern or organizing pneumonia (OP) pattern according to the guidelines for idiopathic interstitial pneumonias (IIPs) [25, 27]. Patterns that could not be classified as NSIP or OP were categorized as unclassifiable pattern (S2 Protocol). Disagreements regarding HRCT interpretation were resolved by consensus between the two radiologists.

Review of pathological findings

Surgical lung biopsy specimens obtained from at least two sites in each patient were reviewed. The pathological classification (UIP, NSIP, or OP) was based on the guidelines for IPF and IIPs [25–27]. Pathological patterns that could not be classified according to these criteria were categorized collectively as an unclassifiable interstitial pneumonia pattern [27].

Each of the following pathological findings was scored semiquantitatively (absent, 0; mild, 1; moderate, 2; and severe, 3): fibroblastic foci, alveolar wall fibrosis, alveolar wall inflammation, intra-alveolar cellularity, and organization. The presence or absence of the following findings was also evaluated: microscopic honeycombing, prominent plasmacytes, dense perivascular collagen, lymphoid aggregate with germinal center, and extensive pleuritis [30, 31].

Pathological patterns and the scoring of pathological findings were evaluated independently by two lung pathologists and the final diagnoses were made by consensus.

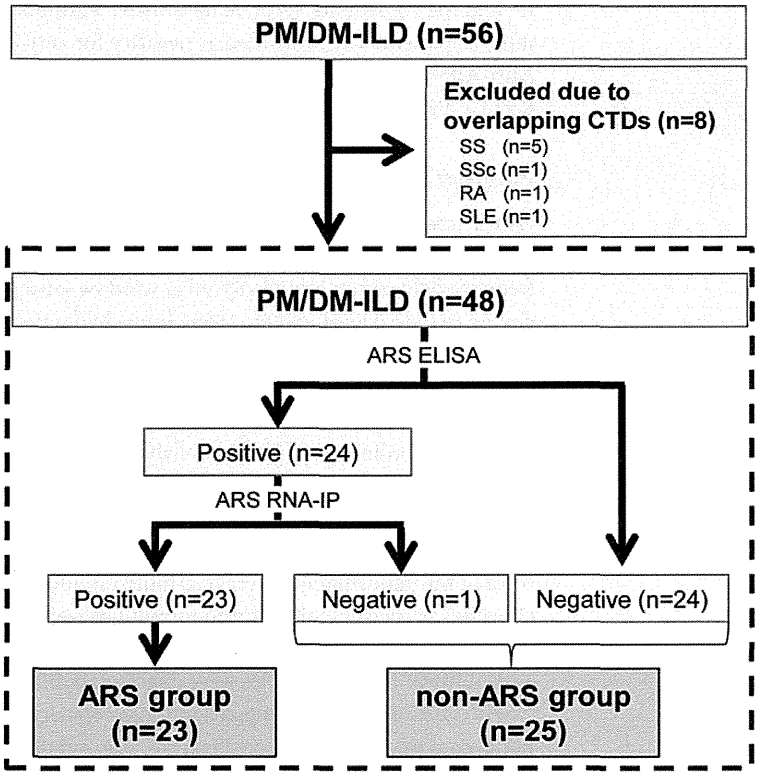

Fig 1. Number of patients included in this study and disease classification. Of 56 patients identified, 8 patients were excluded because of comorbid connective tissue diseases (CTDs) (5 patients with Sjögren's syndrome, 1 with systemic sclerosis, 1 with rheumatoid arthritis, and 1 with systemic lupus erythematosus). There were no patients who had active malignancies at initial diagnosis. Finally, 48 PM/DM-ILD patients were included in this study. PM, polymyositis; DM, dermatomyositis; ILD, interstitial lung disease; CTD, connective tissue disease; SS, Sjögren syndrome; SSc, systemic sclerosis; RA, rheumatoid arthritis; SLE, systemic lupus erythematosus; ELISA, enzyme-linked immunosorbent assay; RNA-IP, RNA immunoprecipitation.

doi:10.1371/journal.pone.0120313.g001

Statistical analysis

All values are expressed as median (range) or number (%). Depending on the sample size, either the Fisher's test or chi-square test was used for comparing proportions among groups. The Mann—Whitney U test was used for comparing medians. Interobserver agreement on HRCT diagnosis was analyzed using the κ statistic test and classified as follows: poor (κ = 0–0.20), fair (κ = 0.21–0.40), moderate (κ = 0.41–0.60), good (κ = 0.61–0.80), and excellent (κ = 0.81–1.00). The observation period for survival was calculated from the date of initial diagnosis of ILD (not PM/DM diagnosis) to the last visit or the time of death. Survival was evaluated using the Kaplan—Meier method and survival curves were compared by the log-rank test. Cox hazards analysis was used to identify variables associated with survival. In all analyses, $P < 0.05$ was considered statistically significant. All data were analyzed using commercially available software (JMP version 9.0.3a, SAS Institute Inc, Cary, NC, USA).

Table 1. Patient characteristics.

	ARS, n = 23	non-ARS, n = 25	*P* value
Median age, yeas (range)			
at ILD diagnosis	55 (37–76)	55 (32–75)	0.66
at PM/DM diagnosis	54 (38–76)	55 (32–75)	0.56
Females, n (%)	19 (82.6)	12 (48.0)	0.017*
Smoking status, n (%)			0.21
Never	15 (65.2)	14 (56.0)	
Former	2 (8.7)	7 (28.0)	
Current	6 (26.1)	4 (16.0)	
Disease onset type			0.17
ILD-preceding	5 (21.7)	2 (8.0)	
Concomitant onset	15 (65.2)	22 (88.0)	
PM/DM-preceding	3 (13.0)	1 (4.0)	
ILD form			0.15
Acute/subacute	7 (30.4)	13 (52.0)	
Chronic	16 (69.6)	12 (48.0)	
IIM type			0.18
PM	1 (4.3)	5 (20.0)	
DM	8 (34.8)	10 (40.0)	
CADM	14 (60.9)	10 (40.0)	
Median observation period, years (range)	5.7 (1.1–12.7)	3.6 (0.2–19.2)	0.16

Data are presented as n (%), median (range).

*$P < 0.05$

ILD, interstitial lung disease; IIM, Idiopathic inflammatory myopathy; PM, polymyositis; DM, dermatomyositis; CADM, clinically amyopathic dermatomyositis.

doi:10.1371/journal.pone.0120313.t001

Results

Clinical characteristics

The clinical characteristics of the ARS and non-ARS groups are summarized in Table 1. The proportion of females was significantly higher in the ARS group than in the non-ARS group (82.6% vs. 48.0%, $P = 0.017$). There were no statistically significant group differences in age at ILD or PM/DM diagnosis, smoking status, disease onset type, ILD form, IIM type, or observation period.

Clinical symptoms, laboratory findings, pulmonary function test results, and BAL findings

The clinical symptoms, laboratory findings, pulmonary function test results, and BAL findings at ILD diagnosis are presented in Table 2. Muscle weakness/myalgia was more frequently observed in the non-ARS group than in the ARS group (52.4% vs. 17.4%, $P = 0.02$). Median CK and aldolase levels were significantly higher in the non-ARS group than the ARS group ($P = 0.017$ and $P = 0.013$, respectively). Median PaO_2 level was significantly lower in the non-ARS group than in the ARS group ($P = 0.04$). Percent predicted forced vital capacity (%FVC) was moderately low in both groups with no significant group difference.

Table 2. Clinical symptoms, laboratory findings, pulmonary function test results, and bronchoalveolar lavage findings at ILD diagnosis.

	ARS, n = 23	non-ARS, n = 25	*P* value
Clinical symptom, n (%)			
Cough	15 (65.2)	13 (52.0)	0.39
Dyspnea on exertion	11 (47.8)	14 (56.0)	0.77
Muscle weakness/Myalgia	4 (17.4)	13 (52.0)	0.02*
Laboratory findings, median (range)			
CK, IU/L	87 (30–798)	281 (24–5274)	0.017*
Aldolase, IU/L	5.6 (3.1–19.1)	11 (3.3–133)	0.018*
KL-6, U/mL	962 (422–3250)	759 (254–2450)	0.81
PaO_2, Torr	80 (63–105)	72 (47.9–103)	0.04*
Pulmonary function tests, median (range)			
FVC, % predicted	66.5 (42.5–93.0)	65.9 (40.6–107.7)	0.99
$FEV_{1.0}$/FVC, %	83.1 (68.1–73.7)	85.4 (73.7–105)	0.22
BAL findings, median (range)			
Lymphocytes, %	10.7 (1.2–70.0)	6.4 (0.6–32.0)	0.26
Neutrophils, %	0.7 (0–14.0)	0.6 (0–31.6)	0.33
Eosinophils, %	2.0 (0–10.2)	0.8 (0–18.6)	0.08
CD4/8 ratio	0.51 (0.07–4.97)	0.66 (0.05–3.82)	0.85

Data are presented as n (%), median (range).

*$P < 0.05$

CK, creatine kinase; PaO_2, arterial oxygen pressure; FVC, forced vital capacity; $FEV_{1.0}$, forced expiratory volume 1.0(sec); BAL, bronchoalveolar lavage.

doi:10.1371/journal.pone.0120313.t002

HRCT distributions, findings, and patterns

Chest HRCT images at ILD diagnosis were available for all patients (Table 3). In both the ARS and non-ARS groups, abnormal HRCT findings were predominantly distributed in the lower lung zone and peripheral and/or peribronchovascular region. GGO, traction bronchiectasis, and lower lobe volume loss were frequently observed in both groups, whereas little or no honeycombing was seen in either group. There were no statistically significant differences in the frequencies of specific findings or distributions between groups. HRCT pattern in all patients was inconsistent with UIP pattern. The NSIP pattern was found in 17 ARS group patients (73.9%) but only in 10 non-ARS group patients (40%). Conversely, the unclassifiable pattern was observed in only 6 ARS group patients (26.1%) but in 11 non-ARS group patients (44%). There was a significant difference in pattern between the two groups ($P = 0.02$).

Pathological patterns and findings

Of the 48 patients, 27 underwent SLB. Pathological patterns and findings are shown in Table 4. The pathological patterns of the ARS group patients with available SLB findings (n = 13) included NSIP in 12 (92%) and UIP in 1 (8%), whereas those of the non-ARS group (n = 14) included NSIP in 11 patients (79%), UIP in 2 (14%), and unclassifiable interstitial pneumonia in 1 (7%). There was no statistically significant difference in pathological pattern frequency distribution between the two groups ($P = 0.51$). There were no significant differences in the frequencies of various pathological findings between ARS and non-ARS groups, including fibroblastic foci [4 (30.8%) vs. 2 (14.3%)], microscopic honeycombing [5 (38.5%) vs. 4 (28.6%)], prominent

Table 3. HRCT distributions, findings, and patterns.

	ARS, n = 23	non-ARS, n = 25	*P* value
Cranio-caudal distribution			0.23
Upper predominance	0 (0)	0 (0)	
Lower predominance	23 (100)	22 (88.0)	
Random/diffuse	0 (0)	3 (12.0)	
Axial distribution			
Peripheral	14 (60.1)	20 (80.0)	0.21
Peribronchovascular	14 (60.1)	15 (60.0)	1.00
Diffuse	5 (21.7)	4 (16.0)	0.72
HRCT findings			
Ground-glass opacity	23 (100)	22 (88.0)	0.24
Consolidation	13 (56.5)	14 (56)	1.00
Reticular opacities	9 (39.1)	10 (40.0)	1.00
Honeycombing	0 (0)	1 (4)	1.00
Traction bronchiectasis	21 (91.3)	19 (76.0)	0.25
Nonseptal linear opacities/SCLL	17 (73.9)	15 (60.0)	0.37
Emphysema	1 (4.0)	5 (20.0)	0.19
Lower volume loss	22 (95.7)	21 (84.0)	0.35
HRCT patterns			0.03*
UIP/possible UIP	0 (0)	0 (0)	
NSIP	17 (73.9)	10 (40)	
OP	0 (0)	4 (16)	
Unclassifiable	6 (26.1)	11 (44)	

Data are presented as n (%), median (range).

Interobserver agreement on HRCT distributions, findings, and patterns between both radiologists was fair to good (κ = 0.37–0.79).

*$P < 0.05$

HRCT, high-resolution computed tomography; SCLL, subpleural curve linear line; UIP, usual interstitial pneumonia; NSIP, nonspecific interstitial pneumonia; OP, organizing pneumonia.

doi:10.1371/journal.pone.0120313.t003

plasmacytes [7 (53.8%) vs. 8 (57.1%)], and lymphoid aggregate with germinal center [7 (53.9%) vs. 9 (64.3%)], although organization [6 (46.2%) vs. 10 (71.4%)] tended to be less frequent in ARS group.

Treatment and outcome

Twenty-two of 23 patients in the ARS group (95.7%) and 23 of 25 in the non-ARS group (92.0%) were treated for PM/DM-ILD during the observation period (Table 5). Although there was no statistically significant difference in the treatment regimen between the two groups ($P = 0.22$), ARS group patients exhibited a significantly higher response rate (100% vs. 78.3%, $P = 0.049$). In the ARS group, only 1 of 23 patients died (due to cancer of unknown primary origin) during the observation period (4.4%), whereas 8 of 25 non-ARS patients (32.0%) died during the observation period (6 from respiratory failure, 1 from oropharyngeal cancer, and 1 from rupture of an abdominal aortic aneurism). Both the overall death rate and the death rate from respiratory failure were significantly lower in the ARS group ($P = 0.02$ and $P = 0.02$, respectively). Kaplan—Meier survival curves are shown in Fig. 2. The 5-year and 10-year survival rates were higher in the ARS group than in the non-ARS group (5-year: 100% vs. 69.1%; 10-year: 92.3% vs. 40.8%, P = 0.02 by log-rank test).

Table 4. Pathological patterns and findings.

	ARS, n = 13	non-ARS, n = 14	*P* value
Patterns, n (%)			0.51
NSIP	12 (92)	11 (79)	
UIP	1 (8)	2 (14)	
Unclassifiable	0 (0)	1 (7)	
Score, none/mild/moderate/severe			
Fibroblastic foci	9/4/0/0	12/1/1/0	0.20
Alveolar wall fibrosis	0/5/3/5	0/7/4/3	0.62
Alveolar wall inflammation	0/1/12/0	0/4/10/0	0.33
Intra-alveolar cellularity	0/13/0/0	0/11/3/0	0.22
Organization	7/3/3/0	4/4/6/0	0.38
Prevalence, n (%)			
Microscopic honeycombing	5 (38.5)	4 (28.6)	0.69
Prominent plasmacytes	7 (53.8)	8 (57.1)	0.86
Dense perivascular collagen	1 (7.7)	1 (7.1)	0.95
Lymphoid aggregate with germinal center	7 (53.9)	9 (64.3)	0.70
Extensive pleuritis	1 (7.7)	1 (7.1)	0.95

Data are presented as n (%).

NSIP, nonspecific interstitial pneumonia; UIP, usual interstitial pneumonia.

doi:10.1371/journal.pone.0120313.t004

Univariate analysis revealed that seropositive status for anti-ARS antibodies (HR = 0.34; 95% CI 0.08–0.80; $P = 0.01$) was a favorable prognostic factor. In addition, higher PaO_2 levels at initial ILD diagnosis (HR = 0.93, 95% CI 0.89–0.98; $P = 0.007$) were associated with longer survival, whereas the acute/subacute ILD form was related to poorer prognosis (HR = 3.70, 95% CI 1.59–16.7; $P = 0.001$) (Table 6). There were no significant differences in treatment response and outcome among patients exhibiting each anti-ARS antibody detected by RNA-IP (data not shown).

Table 5. Treatment and outcome.

	ARS, n = 23	non-ARS, n = 25	*P* value
Treatment, yes, n (%)	22 (95.7)	23 (92.0)	0.86
Treatment regimen, n (%)			0.22
Prednisolone alone	10 (45.5)	6 (26.1)	
Prednisolone + Cyclosporin	11 (50.0)	14 (60.9)	
Prednisolone + Cyclophosphamide	1 (4.5)	1 (4.3)	
Prednisolone + Tacrolimus	0 (0)	2 (8.7)	
Improvement by initial treatment, yes, n(%)	22 (100)	18 (78.3)	0.049*
Death during observation period, n (%)	1 (4.4)	8 (32.0)	0.02*
Due to respiratory failure, n (%)	0 (0)	6 (24.0)	0.02*

Data are presented as n (%), median (range).

*$P < 0.05$

doi:10.1371/journal.pone.0120313.t005

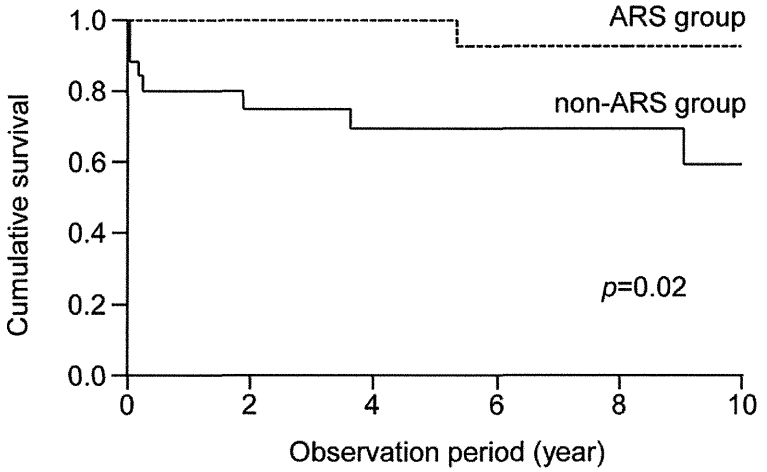

Fig 2. Kaplan—Meier survival curves. The 5-year and 10-year survival rates were higher in the ARS group than in the non-ARS group (5-year: 100% vs. 69.1%; 10-year: 92.3% vs. 40.8%, P = 0.02 by log-rank test).

doi:10.1371/journal.pone.0120313.g002

Discussion

The present study was conducted to elucidate the clinical significance of anti-ARS antibodies in PM/DM-ILD. We found that 48% of PM/DM-ILD patients were positive for anti-ARS antibodies and that these patients showed a female predominance and less frequent myositis compared with non-ARS patients. Radiologically, NSIP pattern was more frequently observed in the ARS group than in the non-ARS group. Furthermore, the presence of anti-ARS antibodies was associated with favorable treatment response and greater survival. To the best of our knowledge, this is the first study to compare the clinical, radiological, and pathological features and clinical outcomes between anti-ARS-positive and anti-ARS-negative PM/DM-ILD patients, providing valuable information for clinical practice.

A previous report showed that a substantial number of patients positive for anti-ARS antibodies were classified as CADM [17]. Consistent with this finding, we observed less frequent

Table 6. Univariate Cox hazards analysis for survival.

	HR	95%CI	*P* value
Anti-ARS-antibodies, positive	0.34	0.08–0.80	0.01*
Sex, female	0.82	0.42–1.65	0.55
Age at ILD diagnosis, years	1.01	0.94–1.08	0.73
Age at PM/DM diagnosis, years	1.01	0.94–1.08	0.80
Never smoked, yes	0.88	0.45–1.78	0.71
ILD form, acute/subacute	3.70	1.59–16.7	0.001*
PaO_2 at initial ILD diagnosis, torr	0.93	0.89–0.98	0.007*
%FVC at initial ILD diagnosis, %	0.95	0.90–1.002	0.06

*$P < 0.05$

HR, hazard ratio; 95%CI, 95% confidence interval; ILD, interstitial lung disease; PM, polymyositis; DM, dermatomyositis; CADM, clinically amyopathic dermatomyositis; PaO_2, arterial oxygen pressure; %FVC, predicted forced vital capacity.

doi:10.1371/journal.pone.0120313.t006

muscle weakness/myalgia and lower serum CK and aldolase levels in the ARS group than in the non-ARS group. Furthermore, patients with CADM were more frequently found in the ARS group than in the non-ARS group (60.9% vs. 40.0%). In accordance with several previous studies showing that ILD often precedes PM/DM diagnosis in patients with anti-ARS antibodies [11, 32], the number of our patients with ILD-preceding type with no evidence of myositis at initial ILD diagnosis was larger in the ARS group than in the non-ARS group (21.7% vs. 8.0%). Collectively, the clinical features of anti-ARS-positive PM/DM-ILD patients were consistent with previous reports.

Radiologically, the NSIP pattern is the most common in PM/DM-ILD [5, 33]. Moreover, OP, diffuse alveolar damage (DAD), UIP, and mixed patterns with these features were also reported [5, 27, 33, 34]. Similar to PM/DM-ILD, the NSIP pattern is likely to be the most common in ASS-ILD, although various other HRCT patterns have also been reported [19–21, 32, 35, 36]. To date, there has been no report comparing HRCT patterns according to the current guidelines for IIPs [26, 27] between anti-ARS-positive and anti-ARS-negative PM/DM-ILD patients. In the present study, the NSIP pattern was significantly more frequent in the ARS group than in the non-ARS group, and HRCT patterns were more heterogeneous in the non-ARS group. Taken together, these results suggest that the presence of anti-ARS antibodies may affect HRCT pattern by influencing disease pathophysiology.

Pathologically, NSIP is also the most common pattern in PM/DM-ILD, followed by UIP and OP [4, 5, 8, 33, 37, 38]. DAD is often encountered in rapidly progressive ILD or autopsy cases [4–8, 33, 37, 38]. In ASS-ILD regardless of PM/DM diagnosis, NSIP is the primary histological pattern [32, 35, 39], but UIP, DAD, and OP are also reported [19–21]. In the present study, NSIP was the predominant pathological pattern in both ARS and non-ARS groups. UIP was pathologically diagnosed in only 8% of ARS and 14% of non-ARS cases, although mild fibroblastic foci and microscopic honeycombing were observed in some cases in this PM/DM-ILD cohort (Table 4). Pathological findings suggestive of underlying CTD [30], such as prominent plasmacytes or lymphoid aggregate with germinal center formation, were present in more than 50% of all PM/DM-ILD patients. There were no significant differences in pathological findings, although organization tended to be more frequent in the non-ARS group. Collectively, our data suggest that PM/DM-ILD patients primarily exhibit the NSIP pattern on lung histology, with no differences in pathological findings between anti-ARS-positive and anti-ARS-negative groups.

Several prognostic factors for PM/DM-ILD have been identified [4, 6–9, 13–15, 34]. Our previous study of 114 patients with PM/DM-ILD indicated that older age, acute/subacute form of ILD, lower FVC, and CADM diagnosis were associated with poor prognosis [9], whereas other reports identified the presence of anti-MDA-5 antibody and higher levels of serum ferritin as indices of poor prognoses [14, 15, 34]. Consistent with previous studies, we found that lower FVC percentage and acute/subacute form of ILD were indicators of poor prognosis in PM/DM-ILD patients. Furthermore, anti-ARS-positive PM/DM-ILD patients (ARS group) had better prognosis compared with anti-ARS-negative PM/DM-ILD patients (non-ARS group) as evidenced by Kaplan—Meier survival curves and Cox hazard analysis. Moreover, the response to the initial treatment was more favorable in the ARS group than in the non-ARS group. Thus, our data suggest that the presence of anti-ARS antibodies predicts better outcome as well as favorable response to the initial treatment in PM/DM-ILD patients.

It was suggested that the clinical features and prognosis may differ depending on the specific types of anti-ARS antibodies present in patients with ASS regardless of the CTD diagnosis [17, 18]. However, we could not find any clinical differences in our PM/DM-ILD cohort, possibly because of relatively smaller sample size (data not shown).

This study had several limitations. First, given its retrospective design and inclusion of ILD patients who visited a pulmonary division, it is subject to several possible biases. For instance, because the current authors' institution is a regional referral center for ILD, referral or selection bias may have increased the number of patients with pulmonary manifestations. Second, because of the relatively small sample size, it was not possible to test whether the identified factors were independent risk factors by multivariate analysis in a Cox proportional hazards model. Third, it is possible that patients positive for anti-OJ antibody (or other anti-ARS antibodies not detected by ELISA) may have been included in the non-ARS group. However, the prevalence of these other anti-ARS antibodies was reported as rare (only 1%–5% of IIM patients) [16, 23]. Thus, it may not have significantly affected our results. Furthermore, MSAs other than anti-ARS antibodies were not measured in this study. Therefore, there is a possibility that some patients may have been positive for other MSAs, including anti-MDA-5 antibody, in our PM/DM-ILD cohort. Further study is needed to clarify this issue. Finally, the initial treatment regimen was not uniform. Most patients were treated with prednisolone (0.5–1.0 mg/kg per day) with/without immunosuppressants, such as cyclosporine, cyclophosphamide, or tacrolimus, for PM/DM-ILD. Given the rarity of PM/DM-ILD, it is unlikely that a larger, prospective, and randomized trial will be performed soon.

In conclusion, the present study demonstrated significant associations between the presence of anti-ARS antibodies and certain clinical features of PM/DM-ILD, such as female predominance and mild myositis. More importantly, positivity for anti-ARS antibodies predicted favorable response to treatment and longer survival. Therefore, measurement of anti-ARS antibodies provides important information for appropriate management of PM/DM-ILD patients.

Supporting Information

S1 Protocol. Definition of HRCT findings.
(DOC)

S2 Protocol. Definition of HRCT patterns.
(DOC)

Acknowledgments

We are grateful to S. Mori for technical support with RNA immunoprecipitation measurements.

Author Contributions

Conceived and designed the experiments: HH NE HS TJ TS. Performed the experiments: HH NE MK TF YN NI HS TJ RN YI TM TS. Analyzed the data: HH NE MK TF YN NI HS TJ RN YI TM TS. Contributed reagents/materials/analysis tools: HH NE MK TF YN NI HS TJ RN YI TM TS. Wrote the paper: HH NE TF HS TJ RN YI TM TS.

References

1. Bohan A, Peter JB. Polymyositis and dermatomyositis (first of two parts). N Engl J Med. 1975; 292: 344–347. PMID: 1090839
2. Bohan A, Peter JB. Polymyositis and dermatomyositis (second of two parts). N Engl J Med. 1975; 292: 403–407. PMID: 1089199
3. Sontheimer RD. Would a new name hasten the acceptance of amyopathic dermatomyositis (dermatomyositis siné myositis) as a distinctive subset within the idiopathic inflammatory dermatomyopathies spectrum of clinical illness? J Am Acad Dermatol. 2002; 46: 626–636. PMID: 11907524

4. Marie I, Hachulla E, Chérin P, Dominique S, Hatron PY, Hellot MF, et al. Interstitial lung disease in polymyositis and dermatomyositis. Arthritis Rheum. 2002; 47: 614–622. PMID: 12522835

5. Marie I, Hatron PY, Dominique S, Cherin P, Mouthon L, Menard JF. Short-term and long-term outcomes of interstitial lung disease in polymyositis and dermatomyositis: a series of 107 patients. Arthritis Rheum. 2011; 63: 3439–3447. doi: 10.1002/art.30513 PMID: 21702020

6. Won Huh J, Soon Kim D, Keun Lee C, Yoo B, Bum Seo J, Kitaichi M, et al. Two distinct clinical types of interstitial lung disease associated with polymyositis-dermatomyositis. Respir Med. 2007; 101: 1761–1769. PMID: 17428649

7. Suda T, Fujisawa T, Enomoto N, Nakamura Y, Inui N, Naito T, et al. Interstitial lung diseases associated with amyopathic dermatomyositis. Eur Respir J. 2006; 28: 1005–1012. PMID: 16837503

8. Fujisawa T, Suda T, Nakamura Y, Enomoto N, Ide K, Toyoshima M, et al. Differences in clinical features and prognosis of interstitial lung diseases between polymyositis and dermatomyositis. J Rheumatol. 2005; 32: 58–64. PMID: 15630726

9. Fujisawa T, Hozumi H, Kono M, Enomoto N, Hashimoto D, Nakamura Y, et al. Prognostic factors for myositis-associated interstitial lung disease. PLoS One. 2014; 9: e98824. doi: 10.1371/journal.pone.0098824 PMID: 24905449

10. Gunawardena H, Betteridge ZE, McHugh NJ. Myositis-specific autoantibodies: their clinical and pathogenic significance in disease expression. Rheumatology (Oxford). 2009; 48: 607–612. doi: 10.1093/rheumatology/kep078 PMID: 19439503

11. Yoshifuji H, Fujii T, Kobayashi S, Imura Y, Fujita Y, Kawabata D, et al. Anti-aminoacyl-tRNA synthetase antibodies in clinical course prediction of interstitial lung disease complicated with idiopathic inflammatory myopathies. Autoimmunity. 2006; 39: 233–241. PMID: 16769657

12. Love LA, Leff RL, Fraser DD, Targoff IN, Dalakas M, Plotz PH, et al. A new approach to the classification of idiopathic inflammatory myopathy: myositis-specific autoantibodies define useful homogeneous patient groups. Medicine (Baltimore). 1991; 70: 360–374. PMID: 1659647

13. Hoshino K, Muro Y, Sugiura K, Tomita Y, Nakashima R, Mimori T. Anti-MDA5 and anti-TIF1-gamma antibodies have clinical significance for patients with dermatomyositis. Rheumatology (Oxford). 2010; 49: 1726–1733. doi: 10.1093/rheumatology/keq153 PMID: 20501546

14. Nakashima R, Imura Y, Kobayashi S, Yukawa N, Yoshifuji H, Nojima T, et al. The RIG-I-like receptor IFIH1/MDA5 is a dermatomyositis-specific autoantigen identified by the anti-CADM-140 antibody. Rheumatology (Oxford). 2010; 49: 433–440. doi: 10.1093/rheumatology/kep375 PMID: 20015976

15. Gono T, Kawaguchi Y, Satoh T, Kuwana M, Katsumata Y, Takagi K, et al. Clinical manifestation and prognostic factor in anti-melanoma differentiation-associated gene 5 antibody-associated interstitial lung disease as a complication of dermatomyositis. Rheumatology (Oxford). 2010; 49: 1713–1719. doi: 10.1093/rheumatology/keq149 PMID: 20498012

16. Hervier B, Benveniste O. Clinical heterogeneity and outcomes of antisynthetase syndrome. Curr Rheumatol Rep. 2013; 15: 349. doi: 10.1007/s11926-013-0349-8 PMID: 23794106

17. Hamaguchi Y, Fujimoto M, Matsushita T, Kaji K, Komura K, Hasegawa M, et al. Common and distinct clinical features in adult patients with anti-aminoacyl-tRNA synthetase antibodies: heterogeneity within the syndrome. PLoS One. 2013; 8: e60442. doi: 10.1371/journal.pone.0060442 PMID: 23573256

18. Aggarwal R, Cassidy E, Fertig N, Koontz DC, Lucas M, Ascherman DP, et al. Patients with non-Jo-1 anti-tRNA-synthetase autoantibodies have worse survival than Jo-1 positive patients. Ann Rheum Dis. 2014; 73: 227–232. doi: 10.1136/annrheumdis-2012-201800 PMID: 23422076

19. Richards TJ, Eggebeen A, Gibson K, Yousem S, Fuhrman C, Gochuico BR, et al. Characterization and peripheral blood biomarker assessment of anti-Jo-1 antibody-positive interstitial lung disease. Arthritis Rheum. 2009; 60: 2183–2192. doi: 10.1002/art.24631 PMID: 19565490

20. Yousem SA, Schneider F, Bi D, Oddis CV, Gibson K, Aggarwal R. The pulmonary histopathologic manifestations of the anti-PL7/antithreonyl transfer RNA synthetase syndrome. Hum Pathol. 2014; 45: 1199–1204. doi: 10.1016/j.humpath.2014.01.018 PMID: 24767252

21. Schneider F, Yousem SA, Bi D, Gibson KF, Oddis CV, Aggarwal R. Pulmonary pathologic manifestations of anti-glycyl-tRNA synthetase (anti-EJ)-related inflammatory myopathy. J Clin Pathol. 2014; 67: 678–683. doi: 10.1136/jclinpath-2014-202367 PMID: 24891607

22. Sato S, Hoshino K, Satoh T, Fujita T, Kawakami Y, Fujita T, et al. RNA helicase encoded by melanoma differentiation-associated gene 5 is a major autoantigen in patients with clinically amyopathic dermatomyositis: Association with rapidly progressive interstitial lung disease. Arthritis Rheum. 2009; 60: 2193–2200. doi: 10.1002/art.24621 PMID: 19565506

23. Nakashima R, Imura Y, Hosono Y, Seto M, Murakami A, Watanabe K, et al. The multicenter study of a new assay for simultaneous detection of multiple anti-aminoacyl-tRNA synthetases in myositis and

interstitial pneumonia. PLoS One. 2014; 9: e85062. doi: 10.1371/journal.pone.0085062 PMID: 24454792

24. Tanizawa K, Handa T, Nakashima R, Kubo T, Hosono Y, Watanabe K, et al. HRCT features of interstitial lung disease in dermatomyositis with anti-CADM-140 antibody. Respir Med. 2011; 105: 1380–1387. doi: 10.1016/j.rmed.2011.05.006 PMID: 21632230

25. American Thoracic Society; European Respiratory Society. American Thoracic Society/European Respiratory Society International Multidisciplinary Consensus Classification of the Idiopathic Interstitial Pneumonias. Am J Respir Crit Care Med. 2002; 165: 277–304. PMID: 11790668

26. Raghu G, Collard HR, Egan JJ, Martinez FJ, Behr J, Brown KK, et al. ATS/ERS/JRS/ALAT Committee on Idiopathic Pulmonary Fibrosis. An official ATS/ERS/JRS/ALAT statement: idiopathic pulmonary fibrosis: evidence-based guidelines for diagnosis and management. Am J Respir Crit Care Med. 2011; 183: 788–824. doi: 10.1164/rccm.2009-040GL PMID: 21471066

27. Travis WD, Costabel U, Hansell DM, King TE Jr, Lynch DA, Nicholson AG, et al. An official American Thoracic Society/European Respiratory Society statement: Update of the international multidisciplinary classification of the idiopathic interstitial pneumonias. Am J Respir Crit Care Med. 2013; 188: 733–748. doi: 10.1164/rccm.201308-1483ST PMID: 24032382

28. American Thoracic Society. Idiopathic pulmonary fibrosis: diagnosis and treatment. International consensus statement. American Thoracic Society (ATS), and the European Respiratory Society (ERS). Am J Respir Crit Care Med. 2000; 161: 646–664. PMID: 10673212

29. Hansell DM, Bankier AA, MacMahon H, McLoud TC, Müller NL, Remy J. Fleischner Society: glossary of terms for thoracic imaging. Radiology. 2008; 246: 697–722. doi: 10.1148/radiol.2462070712 PMID: 18195376

30. Fischer A, West SG, Swigris JJ, Brown KK, du Bois RM. Connective tissue disease-associated interstitial lung disease: a call for clarification. Chest. 2010; 138: 251–256. doi: 10.1378/chest.10-0194 PMID: 20682528

31. Suda T, Kono M, Nakamura Y, Enomoto N, Kaida Y, Fujisawa T, et al. Distinct prognosis of idiopathic nonspecific interstitial pneumonia (NSIP) fulfilling criteria for undifferentiated connective tissue disease (UCTD). Respir Med. 2010; 104: 1527–1534. doi: 10.1016/j.rmed.2010.04.022 PMID: 20483576

32. Marie I, Josse S, Hatron PY, Dominique S, Hachulla E, Janvresse A, et al. Interstitial lung disease in anti-Jo-1 patients with antisynthetase syndrome. Arthritis Care Res (Hoboken). 2013; 65: 800–808. doi: 10.1002/acr.21895 PMID: 23203765

33. Cottin V, Thivolet-Béjui F, Reynaud-Gaubert M, Cadranel J, Delaval P, Ternamian PJ, et al. Interstitial lung disease in amyopathic dermatomyositis, dermatomyositis and polymyositis. Eur Respir J. 2003; 22: 245–250. PMID: 12952255

34. Tanizawa K, Handa T, Nakashima R, Kubo T, Hosono Y, Aihara K, et al. The prognostic value of HRCT in myositis-associated interstitial lung disease. Respir Med. 2013; 107: 745–752. doi: 10.1016/j.rmed.2013.01.014 PMID: 23485097

35. Kalluri M, Sahn SA, Oddis CV, Gharib SL, Christopher-Stine L, Danoff SK, et al. Clinical profile of anti-PL-12 autoantibody. Cohort study and review of the literature. Chest. 2009; 135: 1550–1556. doi: 10.1378/chest.08-2233 PMID: 19225060

36. Takato H, Waseda Y, Watanabe S, Inuzuka K, Katayama N, Ichikawa Y, et al. Pulmonary manifestations of anti-ARS antibody positive interstitial pneumonia—with or without PM/DM. Respir Med. 2013; 107: 128–133. doi: 10.1016/j.rmed.2012.09.005 PMID: 23137883

37. Douglas WW, Tazelaar HD, Hartman TE, Hartman RP, Decker PA, Schroeder DR, et al. Polymyositis-dermatomyositis-associated interstitial lung disease. Am J Respir Crit Care Med. 2001; 164: 1182–1185. PMID: 11673206

38. Tazelaar HD, Viggiano RW, Pickersgill J, Colby TV. Interstitial lung disease in polymyositis and dermatomyositis. Clinical features and prognosis as correlated with histologic findings. Am Rev Respir Dis. 1990; 141: 727–733. PMID: 2310101

39. Watanabe K, Handa T, Tanizawa K, Hosono Y, Taguchi Y, Noma S, et al. Detection of antisynthetase syndrome in patients with idiopathic interstitial pneumonias. Respir Med. 2011; 105: 1238–1247. doi: 10.1016/j.rmed.2011.03.022 PMID: 21514811

International Immunology, Vol. 27, No. 7, pp. 327–332
doi:10.1093/intimm/dxv001
Advance Access publication 10 January 2015

Experimental myositis inducible with transfer of dendritic cells presenting a skeletal muscle C protein-derived CD8 epitope peptide

Naoko Okiyama[1,2,3,4,5], Hisanori Hasegawa[1], Takatoku Oida[3], Shinya Hirata[1], Hiroo Yokozeki[2], Manabu Fujimoto[5], Nobuyuki Miyasaka[1,6] and **Hitoshi Kohsaka[1,4,6]**

[1]Department of Rheumatology, Tokyo Medical and Dental University (TMDU), Bunkyo-ku, Tokyo 113-8519, Japan
[2]Department of Dermatology, Graduate School of Medical and Dental Sciences, Tokyo Medical and Dental University (TMDU), Bunkyo-ku, Tokyo 113-8519, Japan
[3]Japan Society for the Promotion of Science, Tokyo 102-0083, Japan
[4]Research Center for Allergy and Immunology, RIKEN Yokohama Institute, Yokohama, Kanagawa 230-0045, Japan
[5]Department of Dermatology, Faculty of Medicine, University of Tsukuba, Tsukuba, Ibarakii 305-8575, Japan
[6]Global Center of Excellence Program, International Research Center for Molecular Science in Tooth and Bone Diseases, Graduate School of Medical and Dental Sciences, Tokyo Medical and Dental University (TMDU), Bunkyo-ku, Tokyo 113-8519, Japan

Correspondence to: H. Kohsaka; E-mail: kohsaka.rheu@tmd.ac.jp

Received 29 July 2014, *accepted* 6 January 2015

Abstract

It is suggested that polymyositis, an autoimmune inflammatory myopathy, is mediated by autoaggressive CD8 T cells. Skeletal muscle C protein is a self-antigen that induces C protein-induced myositis, a murine model of polymyositis. To establish a new murine model of myositis inducible with a single CD8 T-cell epitope peptide that derives from the C protein, three internet-based prediction systems were employed to identify 24 candidate peptides of the immunogenic fragment of the C protein and bind theoretically to major histocompatibility complex class I molecules of C57BL/6 (B6) mice. RMA-S cell assay revealed that a HILIYSDV peptide, amino acid position 399–406 of the C protein, had the highest affinity to the H2-K^b molecules. Transfer of mature bone marrow-derived dendritic cells pulsed with HILIYSDV induced myositis in naive B6 mice. This myositis was suppressed by anti-CD8-depleting antibodies but not by anti-CD4-depleting antibodies. Because this myositis model is mediated by CD8 T cells independently of CD4 T cells, it should be a useful tool to investigate pathology of polymyositis and develop therapies targeting CD8 T cells.

Keywords: bone marrow-derived dendritic cell, CD4 T cell, RMA-S cell

Introduction

Polymyositis (PM) is an autoimmune inflammatory myopathy of unknown etiology (1). Immunohistochemical studies showed that CD8 T cells infiltrate the pre-necrotic muscle fibers (2–4) and express perforins (5). These findings argue that cytotoxic CD8 T cells (CTLs) drive the pathology of PM.

We established a murine model of PM, C protein-induced myositis (CIM) (6). Biochemical purification studies showed that skeletal muscle fast-type C protein, a myosin-binding protein in the cross-bridge-bearing zone of A bands of myofibrils, appears to be the main immunopathogenic component of the crude skeletal muscle myosin preparation used for the induction of experimental autoimmune myositis in Lewis rats (7, 8). When C57BL/6 (B6) mice were immunized with each of four overlapping protein fragments (fragment 1, 2, 3 and 4) from human skeletal muscle C protein in Freund's complete adjuvant (CFA), histological findings of the proximal muscles showed that mice immunized with fragment 2 (amino acids: 284–580) developed severer myositis than those with other fragments (6). We also found that immunization of a fragment from murine skeletal muscle C protein, corresponding to fragment 2 of the human C protein, induced myositis in B6 mice as well as fragment 2 of the human C protein (9). Since it should contain an epitope with dominant immunogenicity, we have been using the fragment 2 to induce CIM. In CIM, CD8 T cells as well as expression of β2-microgloburin and perforin are essential for myositis induction (10). This fact argues that

cytotoxicity by CD8 T cells is responsible for CIM as is presumed for PM.

Conventional immunization with protein antigens to evoke CTL responses requires CD4 T cells. Actually, depletion of CD4 T cells before immunization of the C protein fragments inhibited CIM development (6, 10). Here, we identified a CD8 epitope in the murine skeletal muscle C protein fragment to evoke CD4 T-cell-independent peptide-induced myositis. The CD8 T-cell-mediated murine model of myositis will be a tool to develop treatments that address directly CD8 T cells.

Methods

Mice

Female B6 mice at age of 8–10 weeks were purchased from Charles River (Yokohama, Japan). All experiments were carried out under specific pathogen-free conditions in accordance with the ethics and safety guidelines for animal experiments of Tokyo Medical and Dental University and RIKEN.

Candidate peptides

Candidate peptides that bind theoretically to major histocompatibility complex (MHC) class I H2-D^b or K^b were identified with SYFPEITHI (http://www.syfpeithi.de/) based on previous publications on T-cell epitopes and MHC ligands (11, 12), HLA Peptide Binding Predictions (http://www-bimas.cit.nih.gov/molbio/hla_bind/) by Dr Ronald Taylor (BIMAS, CBEL, CIT, NIH, Bethesda, MD, USA) and Dr Kenneth Parker (NIAID, NIH) (13) and NetMHC 3.2 Server (http://www.cbs.dtu.dk/services/NetMHC/) (14, 15). Peptides were synthesized by Custom Peptide Service (Sigma–Aldrich, St Louis, MO, USA).

MHC class I expression assay using RMA-S cells

RMA-S, a mutant lymphoma cell line originating from B6 mice, which lacks a functional MHC-linked transporter with antigen processing-2, expresses reduced levels of MHC class I (16). Addition of exogenous peptides that bind to MHC class I restores its expression. They were analyzed after incubation with each candidate peptide and staining with PE-conjugated anti-MHC class I H2-D^b antibodies (KH95; BD Biosciences, San Jose, CA, USA) or H2-K^b antibodies (AF6-88.5).

Immunization of mice with peptides

B6 mice were immunized with 200 μg of synthetic peptides instead of the C protein fragments with the same adjuvants in the method to induce CIM (6, 9). Some mice were intraperitoneally (i.p.) injected with 50 μg of polyinosinic–polycytidylic acid sodium salt [poly (I:C); Sigma–Aldrich] and 50 μg of agonistic anti-CD40 antibodies (FGK-45).

Transfer of bone marrow-derived dendritic cells presenting immunogenic peptides

Bone marrow-derived dendritic cells (BMDCs), prepared as described previously (17), were incubated with 1 μg ml^{-1} of lipopolysaccharides (LPS) (Sigma–Aldrich) for 24 h to up-regulate MHC class I expression on their surface. Flow cytometry showed that >95% of BMDCs increased expression of MHC class I 24 h after the LPS stimulation. Endogenous peptides on MHC class I of BMDCs were replaced with synthetic peptides at 50 μg ml^{-1} each in the final hour. Two million of the peptide-pulsed or non-pulsed BMDCs were intravenously (i.v.) transferred twice with an interval of 3 days to B6 mice that were intra-dermally (i.d.) injected on the footpads with 100 μl of emulsion containing CFA. Seven days after the first transfer, the histological severities of inflammation in the muscles (hamstrings and quadriceps) were graded as in our previous articles (6, 9). Grade 1: involvement of a single muscle fiber or less than five muscle fibers; grade 2: a lesion involving 5–30 muscle fibers; grade 3: a lesion involving a muscle fasciculus; and grade 4: diffuse, extensive lesions. When multiple lesions with the same grade were found in a single block, a 0.5 point was added to the grade.

Immunohistochemistry staining

Cryostat-frozen serial sections (8 μm) of the muscles (hamstrings and quadriceps) from mice 7 days after the first transfer of BMDCs were fixed in 4% paraformaldehyde and stained with 200 ng ml^{-1} anti-CD4 (RM4-5; BD PharMingen) or 400 ng ml^{-1} anti-CD8a (53-6.7; eBioscience, San Diego, CA, USA) monoclonal antibodies or hematoxylin–eosin. Nonspecific staining was blocked with 0.3% hydrogen peroxide in water and 10% rabbit serum (Sigma–Aldrich) in PBS. The sections were incubated with biotin-labeled anti-rat IgG antibodies (Dako, Glostrup, Denmark) and peroxidase-conjugated streptavidin and then visualized with DAB in substrate buffer (R&D systems, Minneapolis, MN, USA). An isotype control, rat IgG2a, κ (eBR2a; eBioscience), was used as a negative control.

In vivo depletion of CD4 or CD8 T cells

To deplete CD4 T cells from B6 mice, the mice were i.p. injected with 500 μg of purified anti-CD4 monoclonal antibodies (GK1.5) (18) every 4 days. To deplete CD8 T cells from B6 mice, the mice were i.p. injected with 1 mg purified anti-CD8 monoclonal antibodies (53.67.2) (19) for three consecutive days. Ten days after, injection of 500 μg of the same antibodies was repeated following every other day for 7 days. Rat IgGs were used as controls. Less than 0.5% of peripheral blood cells or splenocytes of the treated mice were positive for CD4 and CD8 staining with FACS analysis 10 or 7 days after the first injection of the antibodies.

Statistical analysis

Histological scores were analyzed with the Mann–Whitney *U*-test.

Results and Discussion

Identification of an immunogenic peptide derived from murine skeletal muscle C protein

B6 mice develop CIM when immunized with a fragment (amino acids: 279–574) of the murine skeletal muscle C protein (9). Using three internet-based prediction systems, 12 candidate peptides were selected from the fragment for each H2-D^b and H2-K^b with high affinity scores in common among

the three systems. Actual binding of the individual peptides to MHC class I molecules was studied with an assay using RMA-S cells. RMA-S cells showed the highest up-regulation of MHC class I expression when pulsed with a peptide (amino acids: 399–406; HILIYSDV), which binds theoretically to H2-K^b (Table 1).

Peptide-induced experimental myositis

Galea *et al.* (20) reported that CD8 T-cell cross-competition is governed by peptide–MHC class I stability. To establish a myositis inducible with a single CD8 epitope peptide, B6 mice were immunized with HILIYSDV. We first i.d. injected the peptide in CFA without myositis induction in five mice. It was reported that coligation of CD40 on DCs by CD4 T cells was critical in priming antigen-specific CD8 T cells (21–23). Agonistic anti-CD40 antibodies and poly (I:C) synergized to prime CTLs without CD4 T cells (24, 25). We thus immunized seven B6 mice with HILIYSDV with additional i.p. injections of anti-CD40 antibodies and poly (I:C) but found no myositis. The combination adjuvants including CFA, anti-CD40 agonistic antibodies and poly (I:C) might not exert enough effects to present the muscle antigen to CD8 T cells.

Kawachi *et al.* (26) established an experimental myositis in BALB/c mice after four injections of BMDCs pulsed with pyruvate kinase M1/M2-derived peptides, which bind theoretically to H-2K^d of BALB/c mice, into the inguinal lymph nodes. We next performed a transfer of peptide-presenting BMDCs to B6 mice. BMDCs were prepared and activated with LPS to up-regulate MHC class I and CD40 and produce IL-2 (27). The MHC class I molecules should present endogenous peptides. HILIYSDV was or was not pulsed to replace the endogenous peptides on MHC class I of the activated BMDCs. B6 mice were i.v. transferred with the BMDCs twice. Recently, we showed that myositis development requires both autoaggressive T cells and CFA-induced conditioning of muscle tissues in CIM and proposed a 'seed and soil' model of autoimmune diseases (28). Accordingly, the footpads were treated with i.d. injections of CFA emulsion at the day of the first transfer. The treated mice developed myositis 7 days after the first transfer with histological changes including inflammatory cell infiltration around atrophic or regenerating muscle fibers (Fig. 1A and B). The mice presented higher incidence and severity of myositis than the control mice that were treated with activated BMDC transfer alone (Fig. 1D). Mature BMDCs could substitute the helper effect of CD4 T cells instead of anti-CD40 agonistic antibodies and poly (I:C). When the disease course was followed histologically, we observed that the myositis started to decline 10 days and had disappeared 14 days after the first transfer (Fig. 1E), showing that the myositis is self-limited, as is CIM. This myositis was termed C protein peptide-induced myositis (CPIM). While pyruvate kinase M1/M2 that was used as an autoantigen in the previous report is not expressed specifically by the skeletal muscles (29), HILIYSDV was a skeletal muscle-specific antigen. CPIM should be appropriate to investigate organ-specific reactions.

We found that a few mice transferred with BMDCs without the peptide pulse developed myositis (the incidence, 23%; the severity, 0.29 ± 0.03 in Fig. 1D). In a separate experiment, some mice developed myositis with a few necrotic muscle fibers 7 days after i.d. injections of CFA alone at the footpads. These results suggested that the myositis might be induced by activation of innate immunity in the muscle tissues. It might be due to CFA-induced up-regulation of MHC class I expression on muscle fibers. It was reported that transgenic mice that expressed MHC class I highly on their muscle fibers naturally developed myositis (30). On the other hand, we have never found myositis histologically in the brachial muscles from 12 mice with CPIM that were injected i.d. with CFA at footpads of hind legs. Since the upper limbs were not treated with CFA, this result agrees with the 'seed and soil' model as mentioned above (28). We also found that the histological scores of CPIM mice varied among the experiments, which might depend on the purity and activity of BMDCs.

To determine whether other candidate peptides accelerate CPIM, we selected three candidate peptides (ILTINKCTL, RILTINKCTL and DGGRYQVI) based on the results of the RMA-S cell assay (Table 1). BMDCs pulsed with a mixture of HILIYSDV and the three candidate peptides were transferred twice to mice treated with CFA at the footpads. The

Table 1. Candidate CD8 epitope peptides derived from the C protein fragment

MHC class I	Peptide	Fold change of MFI	MHC class I	Peptide	Fold change of MFI
H2-D^b	SAKLNFLEI	2.09	H2-K^b	SKYVFENV	1.19
	KWFKNGQEI	1.21		HVGRFHKL	0.80
	ILTINKCTL	3.00		DEKCFTEL	1.03
	KWYKNGVEV	1.05		ARYRFKKD	1.03
	VVAGNKLRL	1.00		HILIYSDV	6.13
	KQLEVLQDI	0.97		DGGRYQVI	2.43
	KTSDNSIVVV	1.01		DEGDYTFV	1.10
	KTSDNSIVV	1.21		VLQDIADL	1.01
	NGGQCEAELI	1.00		FVPDGYAL	0.72
	VVVAGNKLRL	0.98		SHVGRFHKL	0.77
	RILTINKCTL	2.46		FVPDGYALS	0.77
	LSAKLNFLEI	1.81		EDGGRYQVI	1.44

The amino acid sequences of 24 candidate peptides are described in single letter codes. Mean fluorescence intensities (MFIs) of the peptide-pulsed RMA-S cells stained with anti-MHC class I H2-D^b or H2-K^b antibodies were compared with MFIs of unpulsed RMA-S cells stained with the same antibodies. Fold changes of MFIs show what times candidate peptide-pulsed RMA-S cells up-regulated MHC class I expression compared with unpulsed RMA-S cells.

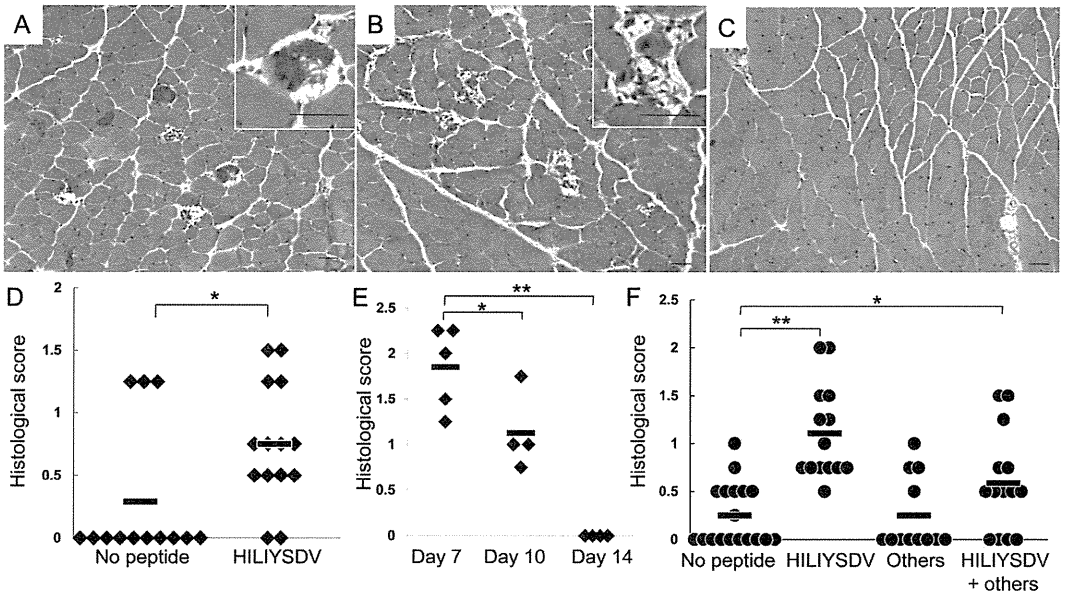

Fig. 1. A CD8 epitope, HILIYSDV, peptide from murine skeletal muscle C protein with a high affinity to MHC class I molecules, induced experimental myositis. A B6 mouse that received BMDCs pulsed with HILIYSDV presented infiltration of inflammatory cells around a few atrophic (A) or regenerating muscle fibers (B) in the femoral muscles, while a B6 mouse that received unpulsed BMDCs did not (C). Bar = 100 μm. (D) The histological scores of the mice that received BMDCs pulsed with HILIYSDV (n = 14) were higher than those of the mice that received unpulsed BMDCs (n = 13). (E) The histological scores of the mice 10 days (n = 4) after the first transfer of BMDCs pulsed with HILIYSDV were reduced compared with those of the mice 7 days after the transfer (n = 5). The myositis had disappeared 14 days after the first transfer in a separate experiment (n = 4). (F) The histological scores of the mice that received BMDCs pulsed with HILIYSDV mixed with three other candidate peptides (n = 14) were lower than those of the mice that received BMDCs pulsed with HILIYSDV (n = 14). The mice that received BMDCs pulsed with the three other peptides (n = 12) barely developed myositis, the same as the mice that received unpulsed BMDCs (n = 18). The rhombus (D, E) or circle (F) symbols and the bars represent the histological scores of individual mice and the average scores of individual groups, respectively. $^{*}P < 0.05$ and $^{**}P < 0.01$.

mice developed myositis with lower incidence and less severity than those treated with transfer of the HILIYSDV-pulsed BMDCs (Fig. 1F). Because mice with transfer of the three candidate peptide-pulsed BMDCs barely developed myositis, the same as those with transfer of unpulsed BMDCs (Fig. 1F), the three peptides are not immunogenic and should have antagonized the effects of HILISDV-inducing CPIM. These results argue that HILIYSDV is a peptide with special immunogenicity to induce experimental myositis without promotional effects of C protein-specific CD4 T cells.

CD4/CD8 T cell dependency of CIM development

Immunohistochemical analyses of the sections of the CPIM muscles revealed that CD8 positive cells infiltrated into the muscle fibers (Fig. 2A). To investigate whether CD8 effector T cells mediate CPIM and whether the helper effects of CD4 T cells are dispensable for the development, the recipient B6 mice were treated with anti-CD4 or CD8 depleting antibodies before the transfer of the HILIYSDV-pulsed BMDCs. While the development of CPIM was not affected by the CD4-positive cell depletion, it was inhibited by the CD8-positive cell depletion (Fig. 2B and C). The results demonstrate that CD8-positive CTLs are pathogenic in CPIM and that CD4 T cells are not required.

Unexpectedly, HILIYSDV-specific cytotoxic reactions were not assessable *in vitro* analyses of CD8 T cells isolated from draining lymph nodes of mice with CPIM. The CD8 T cells were stimulated with HILIYSDV-presenting naive splenocytes or BMDCs *ex vivo* and analyzed with methods including enzyme-linked immunospot assays and flow cytometry assays to detect the interferon-γ production and chromium-51 release assays to measure their cytotoxicities. The difficulties in detecting the *in vitro* CTL activity might be due to small clonal size or weak cytotoxicity of HILIYSDV-specific CTLs in the mice. In this regard, it has been known that no islet autoantigens can induce detectable *in vitro* responses to BDC2.5 autoreactive diabetogenic BDC2.5 T cells.

To address whether HILIYSDV is a dominant epitope in CIM, we treated B6 mice with HILIYSDV in incomplete Freund's adjuvant (IFA) to establish tolerance prior to CIM induction. While injection of C protein fragments in IFA blocked CIM development, that of HILIYSDV did not. Thus, HILIYSDV may not be the dominant CD8 epitope since we screened the peptides based on their affinity to MHC class I molecules. Also, these results do not necessarily argue against the dominant role of the peptide. Tolerance development to C protein by the C protein fragments might depend on tolerance in C protein-specific CD4 T cells because CIM development is mediated by both CD4 and CD8 T cells (6). While systemic or mucosal administration of MHC class II-binding peptides induced tolerance of CD4 T cells in various autoimmune disease models (31–33), peptide-induced tolerance of CD8 T cells has been shown to be limited in antigen-specific T-cell receptor-transgenic mice (34–36) and virus-induced autoimmune diabetes (37, 38). Of most importance is the myositis induction by a CD8 epitope peptide.

CPIM is a new murine model of a CD8 epitope peptide-induced myositis. The peptide, HILIYSDV, derives from the

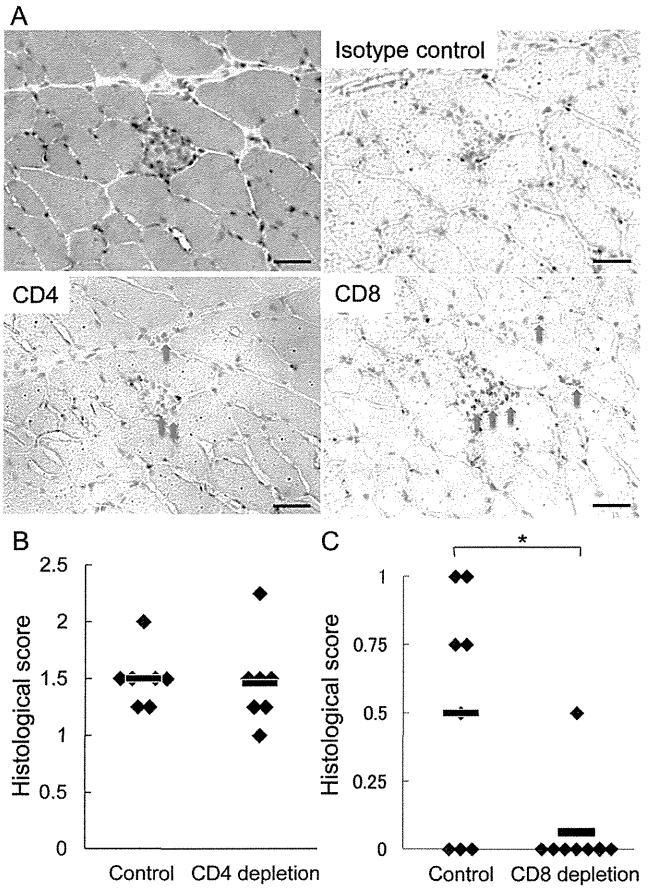

Fig. 2. Sections of muscle from a mouse with CPIM that include necrotizing muscle fiber with infiltrating inflammatory cells (hematoxylin and eosin staining) were immunohistochemically stained with anti-CD4 or anti-CD8 antibodies or isotype control (A). CD8-positive cells infiltrated into the muscle fiber. Data are representative of three mice. Arrows show positive cells. Development of C protein peptide (HILIYSDV)-induced myositis was inhibited by CD8 T-cell depletion but not by CD4 T-cell depletion. Recipient B6 mice were treated with control rat IgGs, anti-CD4-depleting antibodies (B) or anti-CD8-depleting antibodies (C) before the transfer of BMDCs presenting HILIYSDV. $^*P < 0.05$. The rhombus symbols and the bars represent the histological scores of individual mice and the average scores of individual groups, respectively.

murine skeletal muscle C protein and has a high affinity to MHC class I H2-K^b. Because CPIM is mediated by CD8 T cells independently of CD4 T cells, this new model should be a useful tool to investigate pathology of PM and develop treatments targeting CD8 T cells. We have published research showing that blockade of interleukin (IL)-6, IL-1 or tumor necrosis factor-α was effective to treat conventional CIM (9, 39). The target cells of these immunosuppressive agents are unclear. Another experimental myositis that we established, which was induced by an adoptive transfer of T cells from CIM mice to recipient B6 mice, was used to clarify if these agents activated innate immunity in the muscle tissues (28). Experiments using CPIM will clarify whether the immunosuppressive agents directly inhibit the activation of CD8 T cells. Although measurement of muscle weakness in mice is still an unsolved issue, we have established three models of myositis as tools to dissect the pathology of the myositis and to develop specific treatments.

Funding

Ministry of Health, Labour and Welfare; Ministry of Education, Culture, Sports, Science and Technology (MEXT), Japan; Global Center of Excellence (GCOE) Program, 'International Research Center for Molecular Science in Tooth and Bone Diseases'; Japan Society for the Promotion of Science (to N.O.); Shiseido Co.; Japan Rheumatism Foundation.

Acknowledgements

We thank M. Suzuki and E. Yoshimoto for technical assistance. All authors have stated no financial, professional or personal conflict of interest.

References

1 Dalakas, M. C. and Hohlfeld, R. 2003. Polymyositis and dermatomyositis. *Lancet* 362:971.
2 Arahata, K. and Engel, A. G. 1984. Monoclonal antibody analysis of mononuclear cells in myopathies. I: quantitation of subsets according to diagnosis and sites of accumulation and demonstration and counts of muscle fibers invaded by T cells. *Ann. Neurol.* 16:193.
3 Engel, A. G. and Arahata, K. 1984. Monoclonal antibody analysis of mononuclear cells in myopathies. II: phenotypes of autoinvasive cells in polymyositis and inclusion body myositis. *Ann. Neurol.* 16:209.
4 Engel, A. G., Arahata, K. and Emslie-Smith, A. 1990. Immune effector mechanisms in inflammatory myopathies. *Res. Publ. Assoc. Res. Nerv. Ment. Dis.* 68:141.
5 Goebels, N., Michaelis, D., Engelhardt, M. *et al.* 1996. Differential expression of perforin in muscle-infiltrating T cells in polymyositis and dermatomyositis. *J. Clin. Invest.* 97:2905.
6 Sugihara, T., Sekine, C., Nakae, T. *et al.* 2007. A new murine model to define the critical pathologic and therapeutic mediators of polymyositis. *Arthritis Rheum.* 56:1304.
7 Kojima, T., Tanuma, N., Aikawa, Y., Shin, T., Sasaki, A. and Matsumoto, Y. 1997. Myosin-induced autoimmune polymyositis in the rat. *J. Neurol. Sci.* 151:141.
8 Kohyama, K. and Matsumoto, Y. 1999. C-protein in the skeletal muscle induces severe autoimmune polymyositis in Lewis rats. *J. Neuroimmunol.* 98:130.
9 Okiyama, N., Sugihara, T., Iwakura, Y., Yokozeki, H., Miyasaka, N. and Kohsaka, H. 2009. Therapeutic effects of interleukin-6 blockade in a murine model of polymyositis that does not require interleukin-17A. *Arthritis Rheum.* 60:2505.
10 Sugihara, T., Okiyama, N., Suzuki, M. *et al.* 2010. Definitive engagement of cytotoxic CD8 T cells in C protein-induced myositis, a murine model of polymyositis. *Arthritis Rheum.* 62:3088.
11 Rammensee, H. G., Friede, T. and Stevanoviic, S. 1995. MHC ligands and peptide motifs: first listing. *Immunogenetics* 41:178.
12 Rammensee, H., Bachmann, J., Emmerich, N. P., Bachor, O. A. and Stevanović, S. 1999. SYFPEITHI: database for MHC ligands and peptide motifs. *Immunogenetics* 50:213.
13 Parker, K. C., Shields, M., DiBrino, M., Brooks, A. and Coligan, J. E. 1995. Peptide binding to MHC class I molecules: implications for antigenic peptide prediction. *Immunol. Res.* 14:34.
14 Nielsen, M., Lundegaard, C., Worning, P. *et al.* 2003. Reliable prediction of T-cell epitopes using neural networks with novel sequence representations. *Protein Sci.* 12:1007.
15 Lundegaard, C., Lamberth, K., Harndahl, M., Buus, S., Lund, O. and Nielsen, M. 2008. NetMHC-3.0: accurate web accessible predictions of human, mouse and monkey MHC class I affinities for peptides of length 8–11. *Nucleic Acids Res.* 36:W509.
16 Townsend, A., Ohlén, C., Bastin, J., Ljunggren, H. G., Foster, L. and Kärre, K. 2007. Pillars article: association of class I major

histocompatibility heavy and light chains induced by viral peptides. Nature 1989. 340: 443-448. *J. Immunol.* 179:4301.
17 Lutz, M. B., Kukutsch, N., Ogilvie, A. L. *et al.* 1999. An advanced culture method for generating large quantities of highly pure dendritic cells from mouse bone marrow. *J. Immunol. Methods* 223:77.
18 Titus, R. G., Ceredig, R., Cerottini, J. C. and Louis, J. A. 1985. Therapeutic effect of anti-L3T4 monoclonal antibody GK1.5 on cutaneous leishmaniasis in genetically-susceptible BALB/c mice. *J. Immunol.* 135:2108.
19 Mogi, S., Sakurai, J., Kohsaka, T. *et al.* 2000. Tumour rejection by gene transfer of 4-1BB ligand into a CD80(+) murine squamous cell carcinoma and the requirements of co-stimulatory molecules on tumour and host cells. *Immunology* 101:541.
20 Galea, I., Stasakova, J., Dunscombe, M. S., Ottensmeier, C. H., Elliott, T. and Thirdborough, S. M. 2012. CD8+ T-cell cross-competition is governed by peptide-MHC class I stability. *Eur. J. Immunol.* 42:256.
21 Bennett, S. R., Carbone, F. R., Karamalis, F., Flavell, R. A., Miller, J. F. and Heath, W. R. 1998. Help for cytotoxic-T-cell responses is mediated by CD40 signalling. *Nature* 393:478.
22 Ridge, J. P., Di Rosa, F. and Matzinger, P. 1998. A conditioned dendritic cell can be a temporal bridge between a CD4+ T-helper and a T-killer cell. *Nature* 393:474.
23 Schoenberger, S. P., Toes, R. E., van der Voort, E. I., Offringa, R. and Melief, C. J. 1998. T-cell help for cytotoxic T lymphocytes is mediated by CD40-CD40L interactions. *Nature* 393:480.
24 Ahonen, C. L., Doxsee, C. L., McGurran, S. M. *et al.* 2004. Combined TLR and CD40 triggering induces potent CD8+ T cell expansion with variable dependence on type I IFN. *J. Exp. Med.* 199:775.
25 Llopiz, D., Dotor, J., Zabaleta, A. *et al.* 2008. Combined immunization with adjuvant molecules poly(I:C) and anti-CD40 plus a tumor antigen has potent prophylactic and therapeutic antitumor effects. *Cancer Immunol. Immunother.* 57:19.
26 Kawachi, I., Tanaka, K., Tanaka, M. and Tsuji, S. 2001. Dendritic cells presenting pyruvate kinase M1/M2 isozyme peptide can induce experimental allergic myositis in BALB/c mice. *J. Neuroimmunol.* 117:108.
27 Behrens, G., Li, M., Smith, C. M. *et al.* 2004. Helper T cells, dendritic cells and CTL Immunity. *Immunol. Cell Biol.* 82:84.
28 Okiyama, N., Sugihara, T., Oida, T. *et al.* 2012. T lymphocytes and muscle condition act like seeds and soil in a murine polymyositis model. *Arthritis Rheum.* 64:3741.
29 Tsutsumi, H., Tani, K., Fujii, H. and Miwa, S. 1988. Expression of L- and M-type pyruvate kinase in human tissues. *Genomics* 2:86.
30 Nagaraju, K., Raben, N., Loeffler, L. *et al.* 2000. Conditional up-regulation of MHC class I in skeletal muscle leads to self-sustaining autoimmune myositis and myositis-specific autoantibodies. *Proc. Natl Acad. Sci. USA* 97:9209.
31 Gaur, A., Wiers, B., Liu, A., Rothbard, J. and Fathman, C. G. 1992. Amelioration of autoimmune encephalomyelitis by myelin basic protein synthetic peptide-induced anergy. *Science* 258:1491.
32 Critchfield, J. M., Racke, M. K., Zuniga-Pflucker, J. C. *et al.* 1994. T cell deletion in high antigen dose therapy of autoimmune encephalomyelitis. *Science* 263:1139.
33 Tisch, R., Wang, B. and Serreze, D. V. 1999. Induction of glutamic acid decarboxylase 65-specific Th2 cells and suppression of autoimmune diabetes at late stages of disease is epitope dependent. *J. Immunol.* 163:1178.
34 Bercovici, N., Heurtier, A., Vizler, C. *et al.* 2000. Systemic administration of agonist peptide blocks the progression of spontaneous CD8-mediated autoimmune diabetes in transgenic mice without bystander damage. *J. Immunol.* 165:202.
35 Gutermuth, J., Nograles, K. E., Miyagawa, F., Nelson, E., Cho, Y. H. and Katz, S. I. 2009. Self-peptides prolong survival in murine autoimmunity via reduced IL-2/IL-7-mediated STAT5 signaling, CD8 coreceptor, and V alpha 2 down-regulation. *J. Immunol.* 183:3130.
36 Paek, S. Y., Miyagawa, F., Zhang, H. *et al.* 2012. Soluble peptide treatment reverses CD8 T-cell-induced disease in a mouse model of spontaneous tissue-selective autoimmunity. *J. Invest. Dermatol.* 132:677.
37 Aichele, P., Kyburz, D., Ohashi, P. S. *et al.* 1994. Peptide-induced T-cell tolerance to prevent autoimmune diabetes in a transgenic mouse model. *Proc. Natl Acad. Sci. USA* 91:444.
38 von Herrath, M. G., Coon, B., Lewicki, H., Mazarguil, H., Gairin, J. E. and Oldstone, M. B. 1998. *In vivo* treatment with a MHC class I-restricted blocking peptide can prevent virus-induced autoimmune diabetes. *J. Immunol.* 161:5087.
39 Sugihara, T., Okiyama, N., Watanabe, N., Miyasaka, N. and Kohsaka, H. 2012. Interleukin-1 and tumor necrosis factor α blockade treatment of experimental polymyositis in mice. *Arthritis Rheum.* 64:2655.

PLOS | ONE

RESEARCH ARTICLE

The Inhibitory Core of the Myostatin Prodomain: Its Interaction with Both Type I and II Membrane Receptors, and Potential to Treat Muscle Atrophy

Yutaka Ohsawa[1]*, Kentaro Takayama[2], Shin-ichiro Nishimatsu[3], Tadashi Okada[1,4], Masahiro Fujino[1,5], Yuta Fukai[1], Tatsufumi Murakami[1], Hiroki Hagiwara[6], Fumiko Itoh[7], Kunihiro Tsuchida[8], Yoshio Hayashi[2], Yoshihide Sunada[1]*

1 Department of Neurology, Kawasaki Medical School, Kurashiki, Okayama, 701–0192, Japan, **2** Department of Medicinal Chemistry, Tokyo University of Pharmacy and Life Sciences, Hachioji, Tokyo, 192–0392, Japan, **3** Department of Molecular and Developmental Biology, Kawasaki Medical School, Kurashiki, Okayama, 701–0192, Japan, **4** National Research Center for Protozoan Diseases (NRCPD), Obihiro University of Agriculture and Veterinary Medicine, Obihiro, Hokkaido, 080–8555, Japan, **5** Department of Health and Sports Sciences, Faculty of Medical Professions, Kawasaki University of Medical Welfare, Kurashiki, Okayama, 701–0193, Japan, **6** Department of Medical Science, Teikyo University of Science, Uenohara, Yamanashi, 409–0193, Japan, **7** Laboratory of Cardiovascular Medicine, Tokyo University of Pharmacy and Life Sciences, Hachioji, Tokyo, 192–0392, Japan, **8** Division for Therapies against Intractable Diseases, Institute for Comprehensive Medical Science, Fujita Health University, Toyoake, Aichi, 470–1192, Japan

* yosawa@med.kawasaki-m.ac.jp (YO); ysunada@med.kawasaki-m.ac.jp (YS)

OPEN ACCESS

Citation: Ohsawa Y, Takayama K, Nishimatsu S-i, Okada T, Fujino M, Fukai Y, et al. (2015) The Inhibitory Core of the Myostatin Prodomain: Its Interaction with Both Type I and II Membrane Receptors, and Potential to Treat Muscle Atrophy. PLoS ONE 10(7): e0133713. doi:10.1371/journal.pone.0133713

Editor: Vincent Mouly, Institut de Myologie, FRANCE

Received: February 1, 2015

Accepted: June 30, 2015

Published: July 30, 2015

Data Availability Statement: All relevant data are within the paper.

Funding: This work was supported by research grants for Intramural Neurological and Psychiatric Disorders from the National Center of Neurology and Psychiatry (20B-13, 23-5, 26-8); by grants for Comprehensive Research on Disability, Health, and Welfare from the Ministry of Health, Labour, and Welfare of Japan (H20-018); by Grants-in-Aid for Scientific Research from the Japan Society for the Promotion of Science (C-20591013, C-21591101, C-23591261, C-24590363, C-24591281, C-26461285);

Abstract

Myostatin, a muscle-specific transforming growth factor-β (TGF-β), negatively regulates skeletal muscle mass. The N-terminal prodomain of myostatin noncovalently binds to and suppresses the C-terminal mature domain (ligand) as an inactive circulating complex. However, which region of the myostatin prodomain is required to inhibit the biological activity of myostatin has remained unknown. We identified a 29-amino acid region that inhibited myostatin-induced transcriptional activity by 79% compared with the full-length prodomain. This inhibitory core resides near the N-terminus of the prodomain and includes an α-helix that is evolutionarily conserved among other TGF-β family members, but suppresses activation of myostatin and growth and differentiation factor 11 (GDF11) that share identical membrane receptors. Interestingly, the inhibitory core co-localized and co-immunoprecipitated with not only the ligand, but also its type I and type II membrane receptors. Deletion of the inhibitory core in the full-length prodomain removed all capacity for suppression of myostatin. A synthetic peptide corresponding to the inhibitory core (p29) ameliorates impaired myoblast differentiation induced by myostatin and GDF11, but not activin or TGF-β1. Moreover, intramuscular injection of p29 alleviated muscle atrophy and decreased the absolute force in caveolin 3-deficient limb-girdle muscular dystrophy 1C model mice. The injection suppressed activation of myostatin signaling and restored the decreased numbers of muscle precursor cells caused by caveolin 3 deficiency. Our findings indicate a novel concept for this newly identified inhibitory core of the prodomain of myostatin: that it not only suppresses